6-10-2020

# Flomosys: A Flood Monitoring System

Tai Groot

**SANTA CLARA UNIVERSITY**

Department of Computer Science and Engineering

I HEREBY RECOMMEND THAT THE THESIS PREPARED
UNDER MY SUPERVISION BY

Tai Groot

ENTITLED

# Flomosys: A Flood Monitoring System

BE ACCEPTED IN PARTIAL FULFILLMENT OF THE REQUIREMENTS
FOR THE DEGREE OF

**BACHELOR OF SCIENCE**
IN
**COMPUTER SCIENCE AND ENGINEERING**

B. Dezfouli — 06/14/2020

Advisor: Behnam Dezfouli — date

DocuSigned by:
Nam Ling
96CE94A1A83A48A... — 6/16/2020

Department Chair — date

# Flomosys: A Flood Monitoring System

By

Tai Groot

**SENIOR DESIGN PROJECT REPORT**

Submitted to
the Department of Computer Science and Engineering

of

SANTA CLARA UNIVERSITY

in Partial Fulfillment of the Requirements
for the degree of
Bachelor of Science in Computer Science and Engineering

Santa Clara, California

June 10, 2020

## ABSTRACT

The expansion of the Internet of Things (IoT) has led to numerous innovations in the industry, including improvements to existing systems. Disaster prevention and monitoring systems are a prime example of such systems. Every year, there are significant and preventable financial losses, not to mention the safety hazards caused by floods. To warn people ahead of time, it is possible to deploy low-power wireless sensor nodes to send readings across any terrain to a cloud platform, which can perform pattern analysis, prediction, and alert forwarding to anyone's cellular device. In this paper, I propose Flomosys, a low-cost, low-power, secure, scalable, reliable, and extensible IoT system for monitoring creek and river water levels. Although there are multiple competing solutions to help mitigate this problem, Flomosys fills a niche not covered by existing solutions. Flomosys can be built inexpensively with off-the-shelf components and scales across vast territories at a low cost per sensor node. This paper presents the design and implementation of Flomosys as well as real-world test results.

## ACKNOWLEDGEMENTS

This project has been funded by the Santa Clara Valley Water District, the City of San Jose, Santa Clara University's Frugal Innovation Hub, and Cisco Systems. The author would also like to thank all the students that have contributed to the success of this project: Chelsey Li, JB Anderson, Jaykumar Sheth, Michael Cannife, Peter Ferguson, Salma Abdel Magid, Francesco Petrini, Navid Shaghaghi, and Zach Cameron.

Additionally, the author would like to thank Dr. Behnam Dezfouli, for his many hours of hard work and commitment to the project. From meetings and presentations with the city, to pursuing grants, to helping format journal and conference papers, this project would not have succeeded without him.

# Table of Contents

# Table of Figures

# Acknowledgments

This project has been funded by the Santa Clara Valley Water District, the City of San Jose, Santa Clara University's Frugal Innovation Hub, and Cisco Systems. The author would also like to thank all the students that have contributed to the success of this project: Chelsey Li, JB Anderson, Jaykumar Sheth, Michael Cannife, Peter Ferguson, Salma Abdel Magid, Francesco Petrini, Navid Shaghaghi, and Zach Cameron.

Additionally, the author would like to thank Dr. Behnam Dezfouli, for his many hours of hard work and commitment to the project. From meetings and presentations with the city, to pursuing grants, to helping format journal and conference papers, this project would not have succeeded without him.

# Flomosys: A Flood Monitoring System

Tai Groot

Department of Computer Science and Engineering
Santa Clara University
Santa Clara, California
2020

## ABSTRACT

The expansion of the Internet of Things (IoT) has led to numerous innovations in the industry, including improvements to existing systems. Disaster prevention and monitoring systems are a prime example of such systems. Every year, there are significant and preventable financial losses, not to mention the safety hazards caused by floods. To warn people ahead of time, it is possible to deploy low-power wireless sensor nodes to send readings across any terrain to a cloud platform, which can perform pattern analysis, prediction, and alert forwarding to anyone's cellular device. In this paper, the author proposes Flomosys, a low-cost, low-power, secure, scalable, reliable, and extensible IoT system for monitoring creek and river water levels. Although there are multiple competing solutions to help mitigate this problem, Flomosys fills a niche not covered by existing solutions. Flomosys can be built inexpensively with off-the-shelf components and scales across vast territories at a low cost per sensor node. This paper presents the design and implementation of Flomosys as well as real-world test results.

# Table of Contents

# List of Figures

# Chapter 1

# Introduction

Floods are notoriously earth's most frequent and most destructive natural hazard. While flood damage counts in the billions worldwide as is, climate scientists have predicted that with the rise of global warming, flood events will only intensify in number and magnitude over time. Between the years of 1995 and 2015, flooding affected 2.3 billion people, and claimed 157,000 lives across the globe [1]. Since 2000, the US has spent over $107 billion on the damages caused by floods. During the past seventeen years, however, annual damage costs have continued to increase. California's San Francisco Bay Area in particular is facing a grim future. In 2017, San Jose suffered a flooding of the Coyote Creek which amounted to around $100 million in total damage and displaced 14,000 residents [2]. The Bay Area is not alone in its dismal future according to a team of scientists and economists which studied the global impacts of a rising sea level coupled with a growing economy and population. Their reports predict that flood damage worldwide will cost up to $1 trillion per year by 2050.

In this paper, we present the design and development of a *low-power*, *reliable*, *low-cost*, *scalable*, *secure*, and *extensible* flood monitoring system, referred to as *Flomosys*. This system was installed and has been running in California's Bay Area since Summer 2019. Figure 1.1 presents a high-level architectural diagram of Flomosys. The system is composed of three distinct components, Sensor Nodes (referred to as *Nodes*), the *Gateway*, and the *Cloud* platform. A full installation requires at least one instance of each, but can be scaled efficiently to support many Nodes for each Gateway and multiple Gateways per Cloud. Since Nodes typically rely on battery or energy harvesting as their energy source, we design a low-power circuit and also employ software techniques to minimize energy consumption. Nodes communicate with the Gateway using the long-range radio (LoRa) wireless protocol [3]. On top of LoRa, we design and implement a novel encryption and authentication mechanism called HMENC, which is suitable for low-bandwidth, low-power devices. This specialized encryption mechanism requires very little overhead and provides a built-in checksum feature making it more efficient

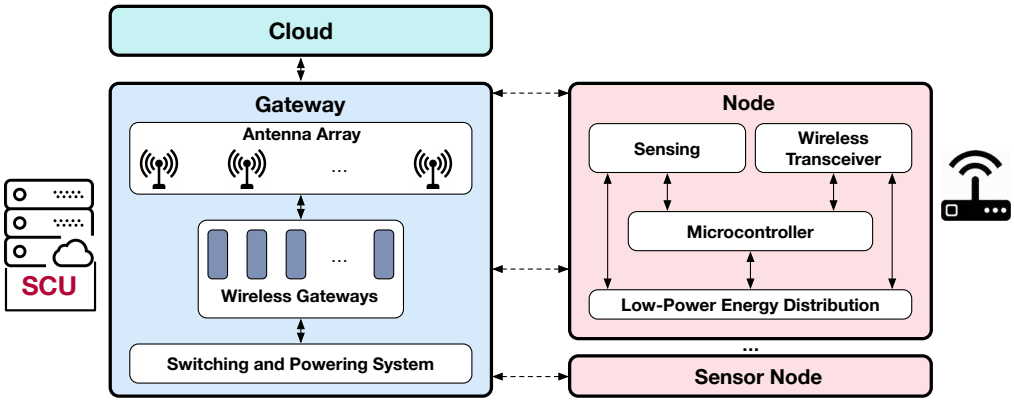


Fig. 1.1: Flomosys architecture. Each Node measures water level and transmits its data over a long-range, secure link to the Gateway. Each Gateway operates on multiple frequencies, perform duplicate packet detection, and forwards the received data to the Cloud. The Cloud provides an administration dashboard for system configuration, as well as data analysis.

than AES or similar general-purpose ciphers, allowing Flomosys to operate using very little energy. In fact, according to our power profiling results, Flomosys should be able to survive between 100 days and almost three years on a 2400 mAh battery, depending on wireless transmission variables (as we will explain in Section 5).

The Gateway design includes an array of receivers connected to directional antennas operating on different frequencies. This provides the Nodes with the diversity required to reach the Gateway in case of link unreliability. Also, the Gateway can be fully implemented using low-cost, single-board Linux devices such as the Raspberry Pi (RPi). If solar or limited energy resources are powering the Gateway, duty-cycling mechanisms are used to reduce its energy consumption [4]. In our current deployment, the Gateway has been installed on the roof of an 11-level tall building belonging to Santa Clara University (SCU).

In addition to reporting water level values to interested agencies, Flomosys can provide endangered residents with proper flood notice. We hope that the designs for this functional system will be freely available for further implementation to aid other flood-prone regions worldwide that suffer frequent losses due to flood damage but have yet to implement robust flood monitoring technology due to financial constraints. For this reason, the Flomosys platform is open-source and is designed to be assembled using commercial off-the-shelf (COTS) components. The source code and hardware designs are published publicly and are freely available, hosted by GitHub on the SIOTLAB's

GitHub account[1]. With this low-cost design, strategic flood precaution is no longer out of reach for impoverished areas and third-world countries. Ultimately, the cost of implementation no longer outweighs the impending costs of flood-related damages.

The rest of this paper is organized as follows: In Chapter 2, we present the system requirements. In Chapter 3, we detail the system architecture and how the different components move data from a Node to the web application. In Chapter 4, we discuss the wireless communication protocols used and the HMENC encryption protocol. In Chapter 5 we examine the power profiling results and explain theoretical system lifetime. In Chapter 6 we discuss related work and how Flomosys fills a new place in the landscape of flood monitoring. We conclude the paper in Chapter 7.

[1]https://github.com/SIOTLAB/Flomosys

# Chapter 2

# Requirements

The major requirements of the system are *reliability*, *energy efficiency*, *scalability*, and *security*.

Concerning *reliability*, in the case of system failures, flood warnings may not reach endangered communities, which is arguably worse than having no system in place at all, as residents may rely on the system. Reliability must be addressed from multiple perspectives. First, the sampled data regarding water height must be accurate. Second, the software managing the operation of Nodes, Gateway, and Cloud platform must always be operational. Third, the Nodes must be able to transmit their data to the Gateway reliably. Fourth, the lifetime of the system components—especially the battery—must be long and predictable.

From the *energy-efficiency* point of view, Nodes may rely on battery or solar harvested energy to recharge their battery. Therefore, it is essential to minimize energy consumption to reduce the cost of an energy harvesting system [5] Relying on renewable energy offers the additional benefit of reducing maintenance costs by eliminating the need to replace batteries frequently.

From the *scalability* point of view, the system must be easy to extend without having to deploy a large number of Gateways. Specifically, since deploying Gateways is more costly and requires permanent Internet access, the ratio of the number of Nodes to the number of Gateways must be a large number.

Last but not least, *secure* communication between Nodes and Gateways is essential. In this regard, authenticity is necessary to ensure a valid Node has generated the data received by a Gateway. Also, integrity is required to ensure the received data is tamper-free. Confidentiality is not essential because the data sampled by Nodes are not confidential.

# Chapter 3

# Architecture and System Overview

At a high level, the system architecture is composed of three components, as Figure 1.1 shows: one or multiple *Nodes*, one or multiple *Gateways*, and a cloud-based coordination and management system, which is simply referred to as the *Cloud*.

## 3.1 Nodes

Figure 3.1 shows a Node's circuitry and packaging. The two major responsibilities of a Node are collecting measurements and sending data packets to the Gateway.

Each Node's sampling rate is adjusted based on several factors, including the last-measured water level and custom settings configured via the Cloud. In the current deployment, during normal operation (i.e., no hazard detected) the sampling interval is within the range of 15 to 30 minutes, depending on a per-node configuration set in the firmware. As the water level increases, the Node's software reduces the sampling interval to ensure timely detection and response. These parameters are configurable via the Cloud platform.

The Node's circuitry includes a microcontroller, wireless transceiver, power distribution circuit, and interface to communicate with an ultrasonic sensor. To reduce the power consumption of the Nodes, several software and hardware optimizations were made. These optimizations allows the Node to achieve a 30 $\mu$A current consumption during sleep mode. The microcontroller used is the ATMEGA328P, which is available on Arduino Pro Mini boards [6]. The software improvements include enabling a low-power mode named "power-down" and disabling all unnecessary functionalities. Specifically, power-down is a power-saving configuration supported by the ATMEGA328P. Power-down mode disables everything except the watchdog timer, TWI Address Match, and interrupts, including pin interrupts. The watchdog timer allows the Node to automatically wake from power-down mode without requiring an external clock or interrupt

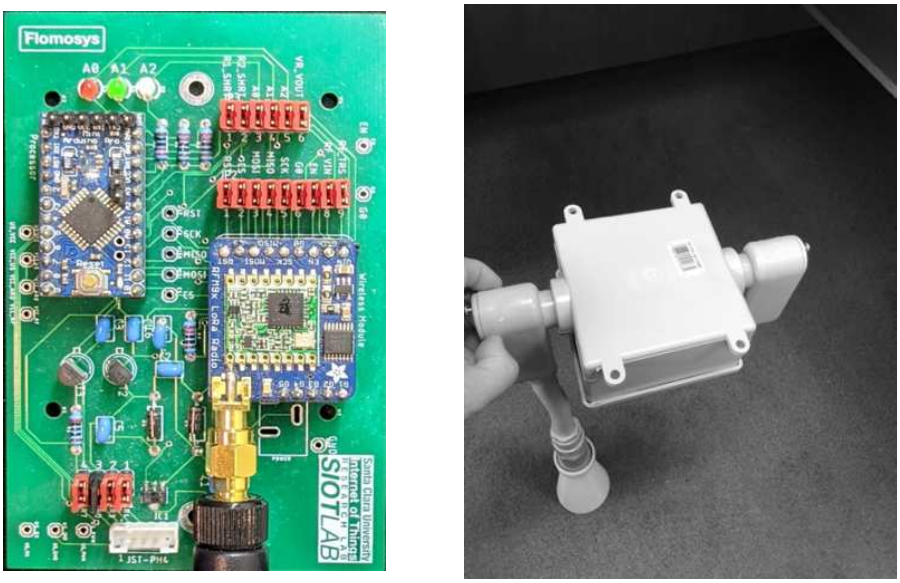


(a) (b)

Fig. 3.1: (a) Node's circuitry, and (b) packaging used for installation. Low-power circuit design and software improvements were employed to ensure minimum power consumption. The current draw of the circuitry during sleep mode is 30 $\mu$A.

trigger. The watchdog periodically generates an interrupt, which transitions the microcontroller from power-down mode to normal operation. If the watchdog wakes the MCU too early, it will revert back to power-down mode until the next timer interrupt, or if it is time to wake, the MCU may remain in normal mode to sample the sensor and transmit data.

Energy efficiency of the circuitry is improved as follows. First, the regulator of the Arduino Pro Mini has been removed. Instead, we use the MCP1703 regulator [7], which has a low-quiescent current of 2 $\mu$A. MCP1703 also allows input voltage within the range 2.7 to 16 V; thereby simplifying interfacing various energy sources such as solar energy harvesting systems. During sleep mode, the microcontroller cuts the power to the wireless transceiver and the ultrasonic sensor to avoid any current leakage. This is achieved by using two on-board transistors. The debugging LEDs (A0-A2) can also be fully disabled by jumpers. We have also removed the onboard LED of the Arduino Pro Mini.

### 3.1.1 Sensor

In addition to energy efficiency, the sensor must provide accurate water level measurements by reporting the distance from the Node itself to the surface of the water. The three main types of distance sensors are ultrasound, LiDAR, and radar. Many LiDAR technologies have issues properly reflecting off water and penetrate the surface instead, leaving radar and ultrasound, both with similar features. Also, ultrasound modules are cheaper than their radar counterparts. Therefore, because ultrasound is affordable, reflects off water properly, and is easy to source from a manufacturing standpoint compared to other technologies, it makes for the ideal distance sensor for Flomosys.

Passive ultrasound sensors send a set of very short pulses and detect the reflection of these signals. A transducer emits these sound pulses, which reflect off objects back to the sensor, and the transducer detects the echoes. The device can then measure the time it takes between the sending and receiving of these pulses. Using this time we can determine the distance between the sensor and the object that has been detected.

### 3.1.2 Control Program

Algorithm 1 presents pseudocode of the program controlling the Node's operation. When a node is awake during its duty-cycle, it first samples using the ultrasonic sensor. Next, it uses HMENC to encrypt the packet, and enters the transmission loop. In the transmission loop, an encrypted packet is transmitted on channel 914 and the node waits for an acknowledgement packet from the base station. If no packet is received before a timeout, the node transmits again on channel 915, and possibly again on 916. This channel hopping helps ensure the node does not violate FCC regulations. Once a packet is received, it is validated. If the packet is too long or short, it is discarded immediately, the retry counter is incremented, and the system attempts to transmit and receive again, provided it has not already retried too many times. If the packet is the right size, it is decrypted and the checksum is calculated. Invalid checksums result in another transmission attempt, retries permitting. Valid checksums result in one of two situations: either the packet is a valid acknowledgement, or it is a seed upgrade. If the packet is an ack, the loop is finished and the node goes into a power-down sleep mode until the duty cycle is finished. Seed upgrades tell the node to update their sequence number and attempt to transmit again, regardless of retries. As this case is very rare,

and the FCC regulations require an "average" dwell time to be lower than 400 ms, an immediate retry every few hundred packets in the event of node reboot is not an issue.

## 3.2 Gateway

A Gateway is responsible for collecting sensor data readings from Nodes, acknowledging the reception of measurements, filtering duplicate receptions, and forwarding data to the Cloud. A Gateway implementation includes multiple Linux-based boards, such as the Raspberry Pi (RPi), where each is connected to a wireless transceiver and antenna. To interface each RPi with a wireless transceiver, we have designed daughter boards that are compatible with RPi header pins. The Gateway was installed on top of a 11-level building belonging to Santa Clara University. The roof of the building was already rented out to several telecommunication providers and therefore has a steady power supply and very fast, reliable internet access.

## 3.3 Cloud

The Cloud Application runs on a managed server hosted on Linode, a hosting service which has a 99.9% uptime SLA, preexisted AWS, and is less expensive than EC2. The Cloud's application itself consists of a front-end and back-end. The API back-end, implemented in Golang, accepts authenticated incoming connections from Gateways streaming measurements and serves requests for the data to the front-end. The front-end, an application written in VueJS, displays several graphs to the user, displaying readings for the previous week, month, and all-time data. An administrator console allows vendors such as water districts to register web-hooks for events such as water level passing a certain threshold. All connections to and from the server are served over TLS with a certificate auto-renewed by LetsEncrypt, a free SSL Certificate Authority (CA). The domain registration is handled through Google Domains, which costs $12 USD per year. Therefore, the total cost to run the cloud services for a year comes to less than $75 USD without requiring expertise with serverless functions.

**Algorithm 1:** Operation of a Node's Controlling Program

```
1  while true do
2      retries = 0;
3      read_ultrasonic();
4      while retries <MAX_PACKET_LISTENS OR time <TIMEOUT do
5          encrypt_packet();
6          transmit_packet();
7          wait_for_ack_packet();
8          if packet length not correct then
9              drop packet;
10             ++retries;
11             continue;
12         else
13             if packet fails checksum then
14                 drop packet;
15                 ++retries;
16                 continue;
17             else
18                 if msg_type == seed upgrade then
19                     if seed packet has correct seq_no then
20                         current_seed = message_seed;
21                         encrypt_packet();
22                         retries=0;
23                         continue;
24                     else
25                         ++retries;
26                         continue;
27                     end
28                 else
29                     // data transmission is successful
30                     break;
31                 end
32             end
33         end
34     end
35     increment_seed();
36     sleep();
37 end
```

# Chapter 4

# Wireless Communication

In this section, we discuss the importance and challenges of wireless communication while designing Flomosys. We also present the details of wireless communication and the security protocol implemented.

## 4.1 Reliable, Long-Range Wireless Links

The choice of wireless technology used has a significant impact in terms of reliability, energy-efficiency, range, and security. We did not choose cellular communication for several reasons. First, cellular service may not be available in remote areas, and it is unreasonable to expect Flomosys end-users to set up their own cell towers in the event of no coverage. Second, cellular communication requires subscription, which increases deployment cost. Although WiFi offers a high data rate and standardized security practices, its range is short and requires access point installation near (∼100 m) each Node. Also, the WiFi communication protocol requires association and maintaining association to allow the Nodes to communication with access points. Both 802.15.4 and Bluetooth Low Energy (BLE) offer energy-efficient communication. However, similar to WiFi, the communication range of both of these technologies is short (∼100 m).

Given the above discussion, the application at hand requires a low-power wide-area network (LPWAN) technology stack. The three main LPWAN technologies in the market are SigFox, Ingenu, and LoRa. We chose LoRa because it satisfies our system requirements in terms of message rate, range, and energy efficiency [8, 9]. LoRa, developed by SemTech, operates in the 915 MHz (North America), 829 MHz (Europe), and 433 MHz (Asia) bands. It has no duty cycle restrictions in North America thanks to its spread-spectrum modulation scheme [10], but a maximum dwell time of 400 ms per channel per 20 second interval is enforced. It can achieve a data rate up to 300 Kbps, but typical data rates are between 300 bps and 27 Kbps, depending on the spreading

factor used. LoRa is unique, with a proprietary hardware stack built to run open source software. The LoRa module that we use is Semtech 1276 [11], which can operate in the 137 MHz to 1020 MHz frequency band. After performing several power profiling tests, such as the one represented in Figure 4.1, it was determined the total energy required to transmit a LoRa packet at +20 dBm with this module ranged from 0.702 Joules to 0.960 Joules, depending on the coding rate and spreading factor.

The same transceiver (Semtech 1276) is used by Nodes as well as the Gateway. The radio control software utilizes Radiohead, an open source RF library licensed under GPLv2 [12]. Each Node is equipped with a directional antenna (mounted on a tall pole near its bridge) pointing toward the Gateway. The current Gateway deployment includes 6 RPi boards. These RPi boards operate on 3 different frequencies with two boards operating on each frequency. This configuration provides redundancy in case of failures. The three frequencies used are 914, 915, and 916 MHz. The transceivers use a spreading factor of 1024 chip-per-second (CPS), a 4/7 coding rate, and have a transmission power of +20 dBm. Each RPi couple is connected to a directional antenna, mounted on a mast installed on the roof of Swig Hall, the tallest building on the campus of Santa Clara University (SCU), at over 11 stories. Figure 4.2 show antennas connected to the Gateway. Together these four antennas span the entire area we need to cover to measure the bridges along Coyote Creek and Guadalupe Creek. We observed reliable coverage extending just over 9 miles away from the Gateway.

## 4.2 Data Security and Integrity

Because the LoRa protocol does not provide any inbuilt encryption or method for secure channel transmission, we have implemented a low-cost data authentication and integrity scheme.

LoRa facilitates the transmission of small packets over a long distance, and the reliability of packet transmission degrades as packet size increases. The data that we need to send is water level, which is represented by a 4-byte variable. Important metadata includes a client ID number to determine which Node is transmitting the reading, and a sequence number, so that duplicate readings can be detected by the Gateway. Duplicate transmissions occur when a Node sends a packet, the Gateway receives it and sends back an ACK, but the ACK is lost; therefore, the Node retransmits the packet. This is demonstrated in Figure 4.4.

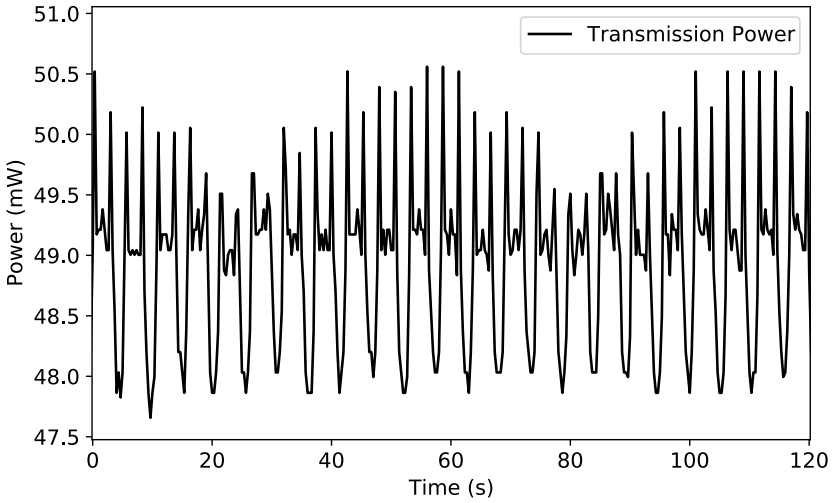


Fig. 4.1: The power required to transmit LoRa packets over time.

Fig. 4.2: Four directional antennas connected to the Gateway. The Gateway has been installed on top of a 11-level building in Santa Clara.

We also added a 2-byte checksum for data validation. After including all the metadata, the message size is 16 bytes.

Such a small packet size is not effectively encrypted with modern encryption algorithms, as they require extra bytes for padding. Typically, using AES-128 would require us to transmit a ciphertext that is a multiple of 16 bytes, which means we are unnecessarily increasing packet size and reducing the chance of a successful transmission.

Additionally, there is a hard limit to the legal transmission length. In the USA, the FCC mandated the maximum dwell time per channel must not exceed 400 ms over any 20

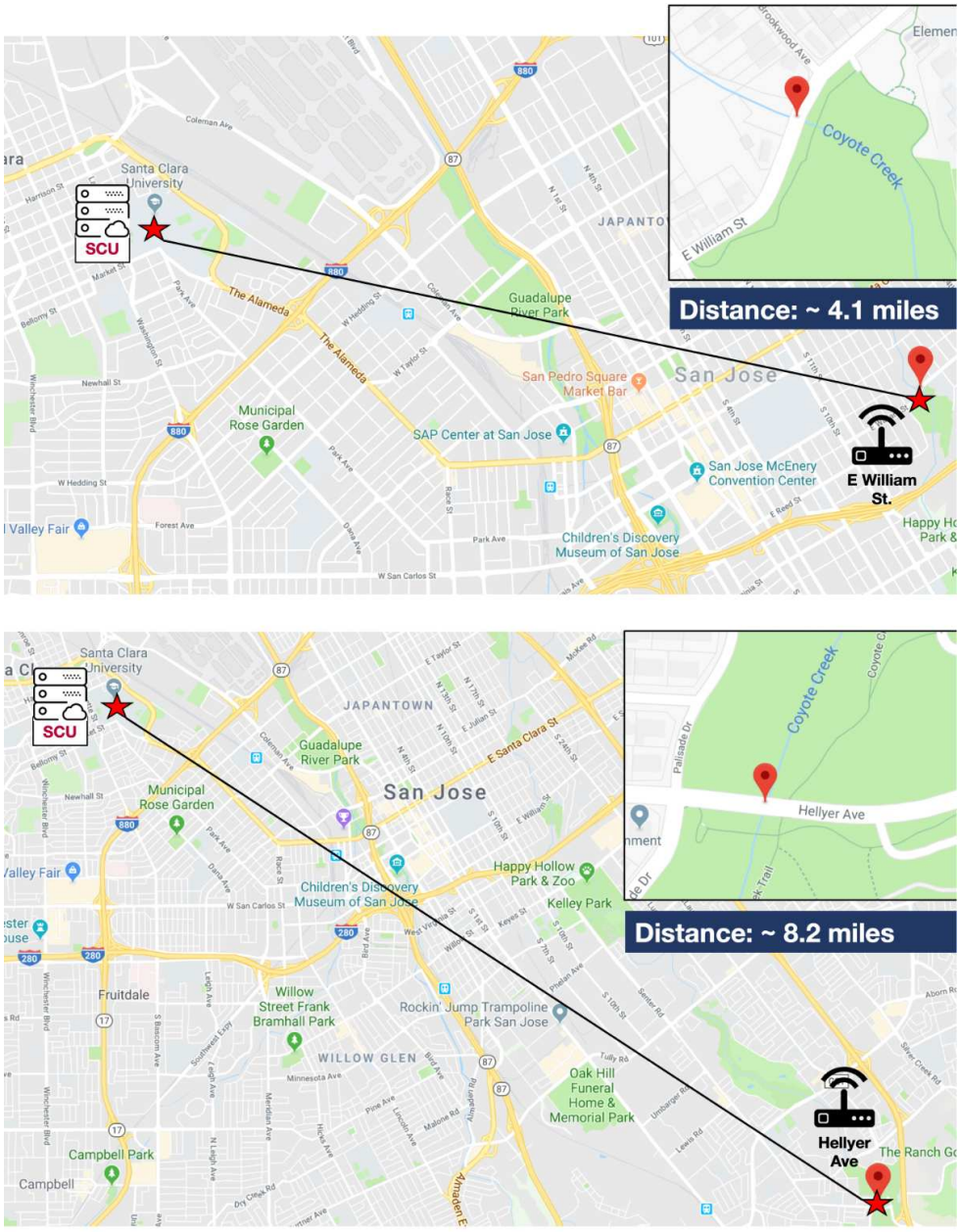


Fig. 4.3: The Gateway and Nodes use directional antennas to improve connectivity. This figure shows two sample locations where the Nodes were placed and their connectivity with the Gateway were tested.

second period. However, to establish stable long-distance links, a high spreading factor and coding rate must be used. These variables significantly increase the time spent transmitting per byte of payload data. Sending 25 bytes or more with a coding rate of

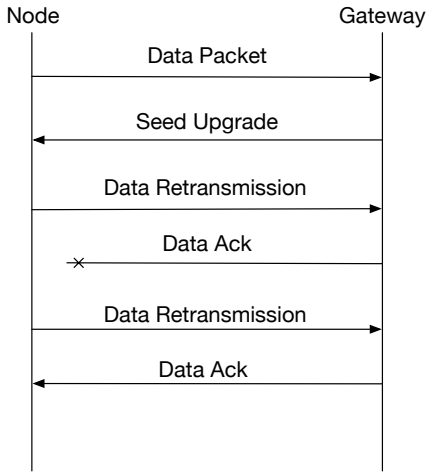


Fig. 4.4: This diagram illustrates three possible cases for message transmission. The first transmission is rejected by the gateway for using an invalid rand_seqno, or seed. The gateway responds with a seed upgrade. The second transmission is received by the gateway, but the ACK message is lost, therefore the Node retransmits the message. Finally, the third transmission is successful and the node receives the ACK sent by the gateway.

4/7 and a spreading factor of 10 results in an illegal transmission rate. Importantly, if the explicit header and CRC are used, there are only 19 usable bytes for the payload section (see Figure 4.5a) of the packet. Similarly, Europe has duty-cycle limitations per channel. As a result, the longer the message sent is, the more infrequent messages must be sent to prevent breaking regulations.

As extra bytes in the total packet size should be avoided to improve transmission reliability, we implemented our own encryption and authentication solution for small data payloads, backed by SHA-2.

## 4.3 HMENC: Low-Power Encryption

HMENC, the encryption solution implemented in Flomosys, uses HMAC and is inspired by the HOTP/TOTP authentication schemes widely in use today for 2-Factor Authentication. The distinction between authentication and confidentiality is important, as generally HTOP/TOTP are only defined for authentication and do not meet the criteria for safe encryption. Additionally, HMENC has not been certified, and although it offers sufficient data confidentiality for Flomosys' use case, the HMENC is better suited to ensure integrity and authenticity. It is important to emphasize that the data pay-

| rand_seqno | client_id | msg_type | seq_no | retries | data | checksum |
|---|---|---|---|---|---|---|
| 44 Bits | 12 Bits | 8 Bits | 8 Bits | 8 Bits | 32 Bits | 16 Bits |

(a) The packet generated by HMENC for float data types. Unencrypted data is filled in gray, and encrypted data is in white. The values in each field represents the number of bits used.

| Preamble | Mandatory Preamble | Explicit (PHY) Headers | Payload | CRC |
|---|---|---|---|---|
| 8 Symbols | 4.25 Symbols | 3 Bytes | 16 Bytes | 2 Bytes |

(b) The physical layer frame used in Flomosys consists of a 2-part preamble, explicit physical headers, the actual data payload, and finally a 2 byte CRC.

Fig. 4.5: (a) Message format. (b) Physical layer frame format.

**Algorithm 2:** Encryption and Integrity Algorithm

```
1 Function encrypt_packet(char message[7], char packet[16]):
2     char checksum[2], pad[9], buffer[9];
3     checksum ⇐ calc_checksum(checksum);
4     pad ⇐ gen_HMAC(rand_seqno);
5     buffer ⇐ message + checksum
6     ciphertext ⇐ buffer ⊕ pad;
7     packet ⇐ rand_seqno + ciphertext;
```

load in this case is extremely small, and only due to this small size does our particular implementation work. As such, HMENC is only defined for small data payloads, such as those under 64 Bytes. Figure 4.5 presents the HMENC message format.

The encryption algorithm is presented in Algorithm 2. Both the Gateway and the Node are preloaded with a shared 32-byte encryption key. Additionally, the gateway maintains a registry of client IDs, which are unique and baked into the Node firmware before deployment. The first time the Nodes are activated, the random number generator is seeded using a static input read from an unused analog pin. Note that it is not critical that this pseudo-random generator be cryptographically random. The random generator fills the first five and a half bytes in a seven-byte array with a pseudo-random sequence number, and the client ID is inserted into the last byte and a half. This seven-byte sequence is used as $m$, the message variable defined by HMAC, and the pre-shared key is used as the HMAC key.

Given

$$K' = \begin{cases} H(K) & K \text{ is larger than block size} \\ K & \text{otherwise} \end{cases}$$

Given $K$, $m$, and $H$, HMAC is defined as follows:

$$HMAC(K, m) = H((K' \oplus opad) \| H((K' \oplus ipad) \| m)) \tag{4.1}$$

where $H$ is a cryptographic hash function (such as SHA-256), $K$ is the key, opad and ipad are magic numbers multiplied by the block size as defined in the HMAC spec, and $m$ is a message, in this case our *random_seqno* [13].

The HMAC algorithm is run and the output is truncated to 9 bytes. This truncated hash is the pad. The message payload is four bytes, long enough to contain a float. The metadata included along with the payload includes a byte for the message type (to allow for future extensibility), one byte for a sequence number, and one byte to hold the number of retries. The two bytes at the end of the plaintext store a two-dimensional checksum value calculated from the rest of the plaintext to verify message authenticity after it is decrypted.

After the metadata, data, and checksum are loaded into a buffer, the plaintext is XORed with the pad, and the *rand_seqno* is prepended to the packet. Lastly, the packet is handed off to the RadioHead LoRa functions for transmission.

Upon receiving a message, the gateway first unpacks the client ID from the 6th and 7th bytes to verify the packet sender is a valid client. Next, the first 7 bytes of the packet are loaded into another buffer and run through the HMAC function along with the pre-shared token to reproduce the pad. The remaining 9 bytes of the packet (the ciphertext) are XORed with the pad to reveal the plaintext. Then, the first 7 bytes of the plaintext are passed through the checksum function, and if the 2-byte checksum matches the checksum provided by the remaining 2 bytes of the plaintext, the packet is determined to be valid. The sequence number is compared to the last seen sequence number. If it is a repeated number, then the gateway will ignore the data but still sends an ACK.

In order to prevent replay attacks, the gateway keeps a list of the last-used `rand_bytes` sequences per node. As `rand_bytes` sequences increase by a constant every message sent, only the last seen sequence per device needs to be remembered.

If a gateway sends a new message with an old random seed (distinguishable from a retransmission thanks to the sequence number), the gateway will respond with a seed upgrade packet. This packet uses the 6 bytes otherwise occupied by the float, sequence number and retries counter to store the first 6 bytes of the rand_bytes the device should use next. The seventh byte is already known, as it is derived from the client ID. This leaves the second half of the 6th byte unused, as it is also occupied by the client id. It is instead set to the value of the invoking packet's sequence number divided by 2, to help mitigate seed upgrade replay attacks. When a device receives this seed upgrade message, it compares the sequence number sent to the sequence number included in the packet. If it is determined to be valid, the Node updates the seed stored in memory to match what the gateway sent, and repacks the original message with the new seed. Therefore, one retransmission is necessary before the data is accepted and processed by the gateway.

The HMENC algorithm is very fast and requires very little energy overhead. Our system profiling shows that the HMENC encryption operation requires approximately 3.28 ms of compute time on a Node. To run these tests, the HMENC code-base was profiled, then modified such that calling the entry-point function immediately returns without any other operations, and profiled again. In Figure 4.6, results from these tests show the cyclical power consumption curve is smoother and shifted higher on the Y-axis, signifying higher energy consumption. Specifically, the baseline tests required 0.071 mJ per operation, and each HMENC encryption required 0.299 mJ per operation. These results were collected using the EMPIOT board [14].

In the end, HMENC requires at least 16 bytes of ciphertext just as AES-128 would, but it offers several benefits over AES. HMENC offers an in-built checksum solution to prevent data corruption, and it allows us to reuse one key across all the devices as no two devices will ever use the same rand_seqno or client id. HMENC allows us to reject packets received by one node but intended for another without decrypting them first, providing speed and therefore power savings. Additionally, if we choose to add features to the device in the future and we must increase our packet size by one byte, we can send a 17-byte packet, whereas using AES-128 would require us to use at least 32 bytes, possibly more depending on how the initialization vector (IV) is generated.

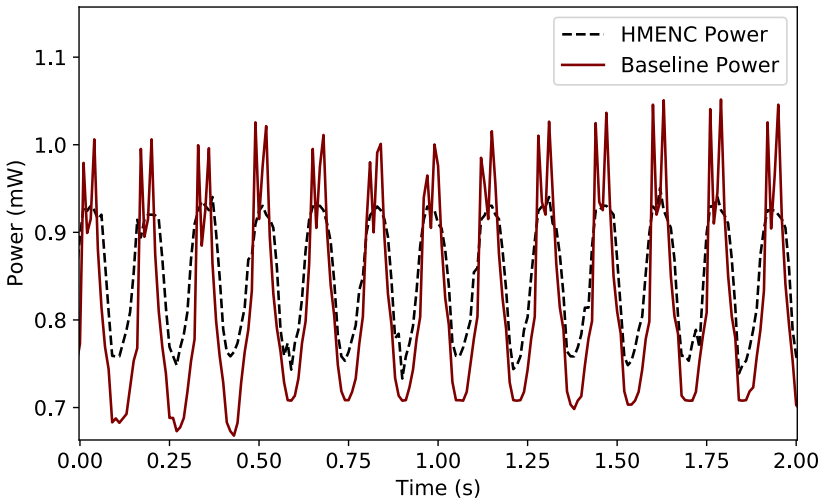


Fig. 4.6: The power consumption of HMENC on Flomosys was compared to a modified HMENC library which returns a constant immediately upon being called to baseline the required power.

# Chapter 5

# Lifetime Analysis

As mentioned in Section 2, energy efficiency is a major concern for Flomosys. Additionally, energy efficiency is directly related to the reliability concerns for the system. As Flomosys is designed for remote locations, often without electricity, it should be feasible to power the system with renewable energy. For example, it should not drain a battery faster than an inexpensive, COTS solar panel is capable of recharging. However, given the many variables involved in calculating expected energy harvest bounties from renewable sources, we have instead chosen to determine how long the system can survive powered by a 2400 mAh battery.

The energy costs for each operation, including data sample collection, packet encryption, and wireless transmission have been recorded and analyzed using the EMPIOT board [14]. These measurements, as well as sleep power consumption were also measured and verified using a high-precision DMM (Tektronix 7510). To determine the theoretical lifetime of Flomosys with different average retries and wireless configurations, we have used the following equation:

$$\begin{aligned} \text{lifetime} &= \frac{E_{bat}}{(E_u + (E_e + E_t) \times (R+1) + E_s) \times N} \\ &= \frac{3600 \times 2400 \times 10^{-3} \times 5}{(E_u + (E_e + E_t) \times R + E_s) \times N} \end{aligned} \tag{5.1}$$

where $E_u$, $E_e$, $E_t$, and $E_s$ are the energy consumption for sampling with the ultrasonic sensor, encrypting a packet, transmitting a packet, and sleeping. $E_{bat}$ is the available energy of the battery, $N$ is the number of cycles per hour, and $R$ is the average number of retries per cycle.

As mentioned in Section 4.2, the most reliable transmission results were observed with a coding rate of 4/7 and a spreading factor of 1024. However, if the Node is closer to the base station, a lower spreading factor and coding rate may be acceptable. For this reason, two graphs have been generated: Figure 5.1a, which displays the theoretical

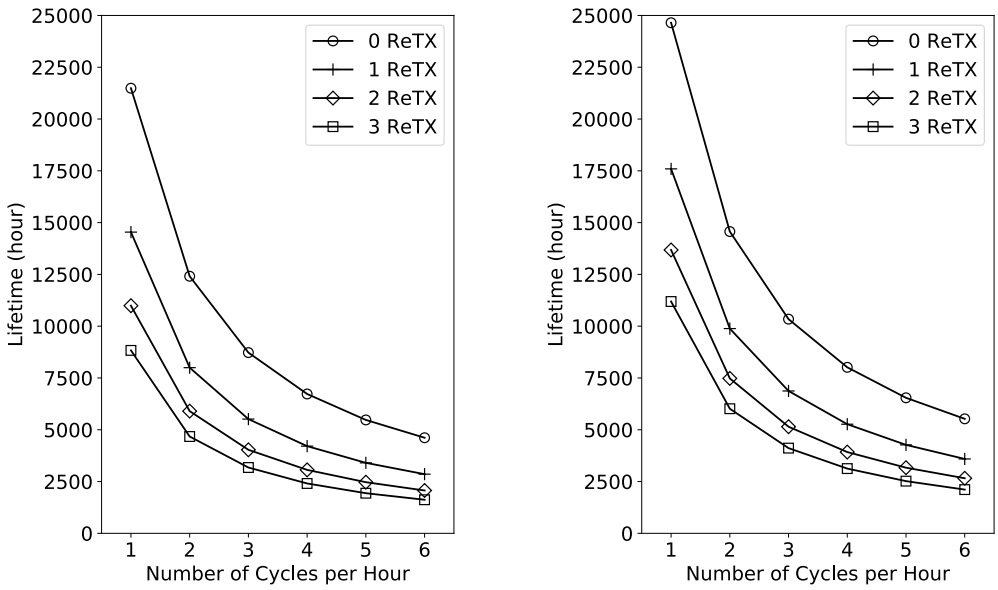


(a) CR: 4/7; SF: 1024 CPS

(b) CR: 4/5; SF: 128 CPS

Fig. 5.1: Theoretical lifetime assuming a 2400 mAh battery with no self-discharge for different average retransmissions, spreading factors (SF), and coding rates (CR).

system lifetime for various retransmission rates at the actual coding rate and spreading factor used, and Figure 5.1b which displays the theoretical system lifetime for various retransmission rates at a lower spreading factor and coding rate, to show maximum lifetime.

Finally, it is important to note these figures do not take into account battery self-discharge, which will significantly lower the system lifetime. The particular battery we use has a lifespan of 5 years [15]. Consequently, the system remains operational for a substantial period before any key component replacement is necessary. Ultimately, the longevity of this component reduces the need for frequent maintenance.

# Chapter 6

# Related Work

The Philippines, which is among the most flood-prone regions in the world, has launched a program that predominantly utilizes LiDAR 3D terrain mapping as well as ultrasonic sensors. The LiDAR technology is coupled with computer-assisted analyses to pinpoint landslide-prone areas, while the ultrasonic sensors are utilized to monitor water levels. More recently, there has been an increased focus on deploying flood warning systems on urban streets. All of these sensors provide data that is analyzed and interpreted, then shared with the public via online flood information websites and mobile device applications.

Another project in the Philippines developed a real-time flood monitoring and early warning system to monitor the water level of the Cagayan River through ultrasonic sensors [16]. This sensor system consists of an Arduino, ultrasonic sensors, a GSM module, web-monitoring software, and SMS-notification hooks to alert stakeholders and mitigate casualties related to flooding.

In 2008, various states in the United States experienced devastating floods [17], including Iowa [18]. This led the University of Iowa to create an Iowa Flood Center (IFC), which was also supported by Tech State of Iowa. IFC has developed many inexpensive river stage (height of water levels above a locally defined reference elevation) sensors which are mounted on bridges to span rivers and streams. They have developed a self-contained and compact Bridge-Mounted River Stage Sensor (BMRSS) [19] for monitoring small rivers and streams, consisting of an ultrasonic distance sensors, a solar panel, a GPS antenna, a heartbeat LED indicator, a cellular modem antenna, and a serial port. In operation, a BMRSS wakes periodically, measures its distance from the water surface and transmits this information via the Internet to IFC servers. They have also developed the Iowa Flood Information System (IFIS) which ingests real time data from BMRSS units and provides a real-time flood monitoring. BMRSS units consist of ultrasonic distance sensor from the Senix Company designed for operation up to 15.2 m (50 ft) with RS-485 interfaces. BMRSS enhances the output from flood forecasting models and

can operate for several years unattended even in harsh environments. As the techniques driven by ultrasonic sensors matured, they have been widely adopted in the various fields of engineering, especially in flood monitoring systems.

Another smart flood monitoring system presented in [20] used the Blynk platform as a medium of data transmission. This system proposes using two NodeMCU development boards connected through Blynk. Blynk is a platform with iOS and Android applications to control an Arduino or Raspberry Pi remotely via the internet [21], providing a digital dashboard to build a graphical user interface with custom widgets. In this project, one NodeMCU is placed at the flood area while the second one acts as the control unit. The transmitter unit consists of a NodeMCU, an ultrasonic sensor, and an LCD display to show the current reading. The data from the ultrasonic sensor is sent to the Blynk application over WiFi, where it is stored in a database and can be transmitted to the internet if the second NodeMCU is connected. This system, using WiFi, has short range especially in urban areas, and deploying nodes on many bridges requires much more hardware than Flomosys, as there is a 1:1 ratio of base stations to nodes, compared to our one-to-many approach.

# Chapter 7

# Conclusion

Multiple competing solutions offer comparable features and use similar methods to monitor flood zones. Unlike the other solutions, Flomosys can be built inexpensively with off-the-shelf components and scales across vast territories at a low cost per Node. In the worst case, Flomosys can continuously report data over long distances over 100 days using a 2400 mAh battery, or for 2.8 years under perfect conditions, marking it as very low-power and energy efficient. HMENC, the low-power encryption algorithm secures all data sent between Nodes and Gateways, and the protocol supports adding new message types in case additional modules need to be added to the board. Together, these properties ensure Flomosys is a low-cost, low-power, secure, scalable, reliable, and extensible flood monitoring solution.

# Bibliography

[1] M. Williams, "2.3 Billion People Affected by Flooding Disasters in 20 Years," https://www.channel4.com/news/factcheck/2-3-billion-people-affected-by-flooding-disasters-in-20-years, 2017.

[2] E. Deruy. (2018) Coyote Creek Victims Sue a Year After Disastrous Flood. https://www.mercurynews.com/2018/02/17/a-year-after-devastating-coyote-creek-floods-some-victims-still-struggling/.

[3] A. Nikoukar, S. Raza, A. Poole, M. Güneş, and B. Dezfouli, "Low-power wireless for the internet of things: Standards and applications," *IEEE Access*, vol. 6, pp. 67 893–67 926, 2018.

[4] I. Amirtharaj, T. Groot, and B. Dezfouli, "Profiling and improving the duty-cycling performance of Linux-based IoT devices," *Journal of Ambient Intelligence and Humanized Computing*, pp. 1–29, 2019.

[5] B. Dezfouli, M. Radi, S. A. Razak, T. Hwee-Pink, and K. A. Bakar, "Modeling low-power wireless communications," *Journal of Network and Computer Applications*, vol. 51, pp. 102–126, 2015.

[6] ATMEL. (2020) ATmega328P Datasheet, 8-bit AVR Microcontroller with 32K Bytes In-System Programmable Flash. [Online]. Available: https://cdn.sparkfun.com/assets/c/a/8/e/4/Atmel-42735-8-bit-AVR-Microcontroller-ATmega328-328P_Datasheet.pdf

[7] MCP1703. [Online]. Available: https://www.microchip.com/wwwproducts/en/en530838

[8] A. Augustin, J. Yi, T. Clausen, and W. M. Townsley, "A study of LoRa: Long range & low power networks for the internet of things," *Sensors*, vol. 16, no. 9, p. 1466, 2016.

[9] F. Adelantado, X. Vilajosana, P. Tuset-Peiro, B. Martinez, J. Melia-Segui, and T. Watteyne, "Understanding the limits of LoRaWAN," *IEEE Communications magazine*, vol. 55, no. 9, pp. 34–40, 2017.

[10] M. Loy, R. Karingattil, and L. Williams, "ISM-band and short range device regulatory compliance overview," *Texas Instruments*, 2005.

[11] Semtech, "Semtech SX1276, 137 MHz to 1020 MHz Long Range Low Power Transceiver," 2017. [Online]. Available: https://www.semtech.com/products/wireless-rf/lora-transceivers/sx1276#download-resources

[12] RH_RF95 Class Reference. [Online]. Available: https://www.airspayce.com/mikem/arduino/RadioHead/classRH__RF95.html

[13] NIST, "FIPS 198-1, The Keyed-Hash Message Authentication Code (HMAC)," NIST, Tech. Rep., Jul 2008. [Online]. Available: https://nvlpubs.nist.gov/nistpubs/FIPS/NIST.FIPS.198-1.pdf

[14] B. Dezfouli, I. Amirtharaj, and C.-C. Li, "EMPIOT: An energy measurement platform for wireless IoT devices," *Journal of Network and Computer Applications*, vol. 121, pp. 135 – 148, 2018.

[15] Tycon Solar. (2018) Outdoor Remote Power Systems, Tycon Solar RPDC Series Data Sheet. http://tyconsystems.com/documentation/Spec%20Sheets/RPDC%20RemotePro_Spec_Sheet.pdf.

[16] J. Natividad and J. Mendez, "Flood monitoring and early warning system using ultrasonic sensor," in *IOP Conference Series: Materials Science and Engineering*, vol. 325, no. 1, 2018.

[17] J. Ambrose, "A watershed year: Anatomy of the iowa floods of 2008 and the 1,000-year flood: Destruction, loss, rescue, and redemption along the mississippi river," *The Annals of Iowa*, vol. 70, no. 2, pp. 191–194, 2011.

[18] Senix, "Water Level Sensors Provide Real-time Flood Warnings in Iowa," https://senix.com/2015/04/29/sensors-provide-iowa-flood-warnings/, 2015.

[19] A. Kruger, W. F. Krajewski, J. J. Niemeier, D. L. Ceynar, and R. Goska, "Bridge Mounted River Stage Sensors (BMRSS)," *Materials Science and Engineering*, vol. 4, 2016.

[20] N. A. Z. M. Noar and M. M. Kamal, "The development of smart flood monitoring system using ultrasonic sensor with blynk applications," in *IEEE ICSIMA*, 2017, pp. 1–6.

[21] "Democratizing the Internet of Things Blynk," http://www.blynk.io.